X-ray-absorption near-edge structure of transition-metal zinc-blende semiconductors: Calculation versus experimental data and the pre-edge feature

David A. McKeown
Semiconductor Electronics Division, National Institute of Standards and Technology, Building 225, Room A305, Gaithersburg, Maryland 20899

(Received 18 March 1991; revised manuscript received 3 September 1991)

X-ray-absorption near-edge structure (XANES) data were collected for Zn in sphalerite (ZnS), and for Cu and Fe in chalcopyrite ($CuFeS_2$), where all three cations are in nearly identical coordination environments. The data have similar features, except near the edge, where the edge maximum decreases in amplitude, while a pre-edge feature appears and increases in amplitude from Zn to Cu to Fe. The pre-edge feature was previously assigned to a 1*s*-to-3*d* atomic transition for Cu and Fe in the chalcopyrite structure. XANES calculations were performed for all three edges. The multiple- and single-scattering contributions to the calculated edge spectra were scaled down to better fit the experimental data. The conclusions from the calculations indicate that the pre-edge feature in the experimental Cu- and Fe-edge data for chalcopyrite can be due to interference effects from the atomic structure surrounding the absorber, but cannot exclude the possibility that the pre-edge feature is due to atomic bound-state transitions of the absorber.

INTRODUCTION

X-ray-absorption near-edge structure (XANES) is known to be sensitive to both the arrangement of atoms around the absorbing atom, as well as the atomic states of the absorbing atom. Therefore it is not surprising that XANES data, collected on compounds having different arrangements of atoms around the absorbing atom, can have very different features.[1] In this study, XANES data were gathered for three transition metals: Fe and Cu in chalcopyrite ($CuFeS_2$), and Zn in sphalerite (ZnS), where all three cations are in nearly identical atomic environments;[2–4] these atomic arrangements are similar to the zinc-blende-type structures in III-V semiconductors. Since the environments are similar, all interference features in the XANES should be similar, and any change in the XANES should, to first approximation, be due entirely to atomic effects of the absorbing atom. The rationale behind this study is to see if any changes in the near-edge data can be assigned to electronic transitions of the absorbing atom, which may be useful for interpreting XANES of III-V semiconductors, as introduced earlier.[5] The experimental Zn-edge data for sphalerite, and the experimental Cu- and Fe-edge data for chalcopyrite have been presented separately,[6–8] but no comparisons or calculations have been made for all three edges.

EXPERIMENTAL

The chalcopyrite and sphalerite specimens (sample numbers 116 536 and 165 714, respectively) were supplied by the Mineral Sciences Department of the National Museum of Natural History, Smithsonian Institution. The specimens were ground to particles approximately 20 μm in diameter. A single layer of the particles, approximately 25 mm by 50 mm in area, was placed on tape. Fluorescence spectra of the samples were gathered at NIST beam line X23-A2 at the National Synchrotron Light Source with ring conditions near 140 mA and 2.5 GeV. Room-temperature spectra were gathered such that the flat sample surface was at 45° with respect to the incident x rays. Incident x rays covered a 1×15-mm^2 area on the sample. The fluorescent x rays from the sample were detected by a *p-i-n* diode[9] positioned normal to the incident x-ray beam, or 45° from the sample. The bean line's Si (220) double crystal monochromator has an energy resolution of approximately 1 eV at the energies measured for this study. The data range in energy from -135 to 615 eV, with the edge energy E_0 defined as 0 eV; the absolute edge energies are 7112 eV (Fe), 8979 eV (Cu), and 9659 eV (Zn). The XANES data range from -20 to 80 eV and were collected in 0.2-eV steps. The spectra presented here were gathered without the use of a harmonic rejection mirror, since the x-ray flux of the synchrotron diminishes by more than 2 orders of magnitude from the first harmonic to the second harmonic for the energy ranges covered by the data. Spectra were gathered with and without a harmonic rejection mirror placed in the path of the incident x rays; there was no distortion in any of the spectra due to higher harmonic x rays in the incident beam for both experimental setups.

DISCUSSION

Data

For each edge, a linear background was fitted to the -135 to -20 eV interval of the data and was then subtracted. All edge steps were normalized to one. The data have similar features, except near the edge, where the edge maximum decreases in amplitude (feature *B* in Fig. 1), while a pre-edge feature appears and increases in amplitude from the Zn edge for sphalerite, to the Cu and Fe

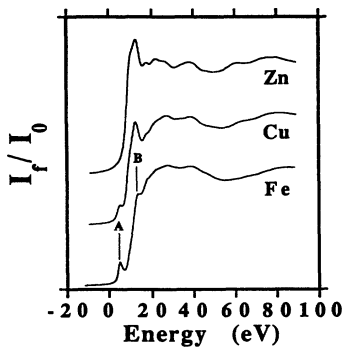

FIG. 1. K-edge data: Zn (sphalerite), Cu and Fe (chalcopyrite). E_0's are shifted to near 0 eV so that similar interference features are at similar energies.

edges for chalcopyrite (feature A in Fig. 1). The pre-edge feature has been assigned to $1s$-to-$3d$ atomic transitions in the absorbing cation.[6] Since, on first thought, the d orbitals become less populated from Zn to Cu to Fe, it would seem logical to have a pre-edge feature appear and grow in amplitude as described above. From the crystal structure determination of ZnS (Ref. 4) and the crystal structure refinement of $CuFeS_2$,[3] valences have been assigned to the cations such that the d orbitals are d^{10} (Zn^{2+}), d^{10} (Cu^+), and d^5 (Fe^{3+}). Due to the covalent nature of the bonding in chalcopyrite, valence states between Cu^+ and Fe^{3+}, and Cu^{2+} and Fe^{2+} have been considered,[3] which may be caused by the hybridization of Fe^{3+} and Cu^+ $3d$ orbitals with S^{2-} $3p$ orbitals. More recent photoemission, Mössbauer, and neutron diffraction studies of chalcopyrite strongly support the Cu^+ and Fe^{3+} configuration.[10,11] From the conclusion that Cu in chalcopyrite has a filled d shell,[6,10,11] the pre-edge feature on the Cu edge for chalcopyrite (feature A in Fig. 1) is unexpected, if it is due to a $1s$-to-$3d$ transition.

Beyond the edge, the interference features for all three spectra are similar (Fig. 1). Interference amplitudes are damped from Zn to Cu and Fe; this damping may be due to the site symmetries being lowered from perfect tetrahedra for Zn in sphalerite, to tetragonally shortened tetrahedra for Cu and Fe along the c axis in chalcopyrite.

Calculations

The calculations were carried out in four different stages: (1) constructing electron charge densities for the cations and anions of interest, (2) generating muffin-tin potentials from the electron charge densities and the coordinating atomic environments of interest, and splicing together the muffin-tin potentials to form pseudomolecular potentials, (3) generating phase shifts and dipole matrix elements from the pseudomolecular potentials (XANES3 program), and (4) performing the full scattering calculation on an atom cluster simulating the crystal structure of interest, which generates the calculated x-ray absorption spectrum (ICXANES program). This method was reviewed by Bunker.[12]

Electron charge densities for Zn^{2+} with a core hole ($1s^1 2s^2 2p^6 3s^2 3p^6 3d^{10} 4s^0$), Cu^+ with a core hole ($1s^1 2s^2 2p^6 3s^2 3p^6 3d^{10} 4s^0$), Fe^{3+} with a core hole ($1s^1 2s^2 2p^6 3s^2 3p^6 3d^5$), and S^{2-}($1s^2 2s^2 2p^6 3s^2 3p^6$) were constructed using a version of the Herman-Skillman self-consistent-field Hartree-Fock-Slater calculations[13] modified to include a variable exchange-correlation parameter α. The α values were taken from Schwartz.[14]

From the electron charge densities generated, muffin-tin potentials were constructed for clusters that contain five atoms which simulate the coordination environments of Zn in sphalerite, and Cu and Fe in chalcopyrite. Muffin-tin potentials were calculated for atom clusters containing Zn^{2+} coordinated by four S^{2-} in tetrahedral symmetry to form a ZnS_4^{6-} cluster, Cu^+ coordinated by four S^{2-} in tetrahedral symmetry to form a CuS_4^{7-} cluster, and Fe^{3+} coordinated by four S^{2-} in tetrahedral symmetry to form a FeS_4^{5-} cluster. The coordinates of the ZnS_4^{6-} cluster are listed in Table I; for this cluster, the Zn-S distance is 2.35 Å.[4] The CuS_4^{7-} and FeS_4^{5-} clusters used the same configuration as the ZnS_4^{6-} cluster, except the coordinates were scaled to have the Cu-S and Fe-S bond distances 2.30 and 2.25 Å, respectively, as in the chalcopyrite structure.[3] The CuS_4^{7-} and FeS_4^{5-} clusters used are undistorted tetrahedra, which are approximations to the slightly distorted CuS_4^{7-} and FeS_4^{5-} tetrahedra in the chalcopyrite structure. The muffin-tin potentials generated for the atoms in these environments were cut off at approximately half of the bond distance between the cation and the S^{2-}, and were then spliced together, using a generalization of the Mattheiss prescription;[15] this removes unphysical discontinuities in the resulting pseudomolecular potential. The methods used for the potential constructions are very simple, and are only rough approximations to the actual bonding in the materials of interest.

The pseudomolecular potentials were input for the XANES3 program, which generated the dipole matrix elements for the absorbing cations of interest, the partial-wave phase-shift functions for both the central cations and the backscattering coordinating ions, and the backscattering amplitudes for the coordinating ions. The XANES3 program generates the atomic contribution to the x-ray-absorption cross section, or the μ_0 of the absorbing atomic species, where one can see effects on the edge shape with respect to changes in the atomic configuration of the absorber, or to changes in the construction of the pseudomolecular potential. For the FeS_4^{5-}, CuS_4^{7-}, and ZnS_4^{6-} environments, the calculated μ_0 edge becomes narrower and develops a sharp maximum as the atomic number of the absorbing cation increases (Fig. 2). No sharp resonances are observed in the phase shifts or backscattering amplitudes for any of the atomic species, that

TABLE I. Coordinates used for the ZnS_4^{6-} cluster to generate muffin-tin potentials.

Atom	x (Å)	y (Å)	z (Å)
Zn^{2+}	0.0	0.0	0.0
S^{2-}	1.923	0.0	1.358
S^{2-}	−1.923	0.0	1.358
S^{2-}	0.0	1.923	−1.358
S^{2-}	0.0	−1.923	−1.358

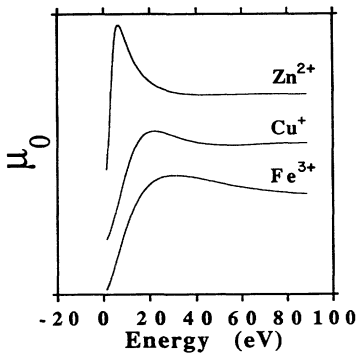

FIG. 2. Calculated μ_0's, or atomic contributions to the absorption spectrum for the ZnS_4^{6-} (sphalerite), CuS_4^{7-} and FeS_4^{5-} (chalcopyrite) cluster pseudomolecular potentials.

may cause enhanced scattering in the energy range near the edge of the calculated spectra. The dipole matrix elements, the partial-wave phase-shift functions, and the scattering amplitudes are then input for ICXANES,[16] which calculates the K-edge spectrum.

Calculations on zinc-blende-structure clusters up to six shells (70 atoms) were performed using ICXANES, where multiple-scattering (MS), single-scattering (SS), and atomic-absorption (μ_0) contributions to the calculated spectra have been determined. The edge steps for all calculated spectra were normalized to one. For the ICXANES calculations, only one polarization orientation of the x rays (parallel to the cluster's z axis or the crystal structure's c axis) is presented here for each cation site, since site symmetries are tetrahedral or nearly tetrahedral. The Cu and Fe sites in chalcopyrite have the tetragonal shortening along the crystal structure's c axis. As a check, a spectrum was calculated for the Fe site, having the x-ray polarization perpendicular to the c axis. The calculated Fe-edge spectra for the two different polarizations show very minor differences. Features in the calculated spectra generally converge as more shells are added. Most edge features in the experimental data are replicated in the two-shell (16-atoms) calculation [for Fe, see Fig. 3(a)]. For all three edges, the five-shell (46-atoms) calculated spectra best match the data; this was also found for the Zn-edge calculations for sphalerite by Sainctavit *et al.*[8] Details of the first five shells around the central absorbing Zn^{2+} in sphalerite, and Cu^{+} and Fe^{3+} in chalcopyrite are given in Table II.

A small peak near the beginning of the edge jump is seen only in the four- and five-shell cluster Fe- [Fig. 3(a) feature A] and Cu-edge calculations. For the Fe-edge calculations, peaks and troughs in the low-energy part of the MS and SS interference functions add constructively [Fig. 3(b), features A and B]; this is the cause of features A and B on the calculated Fe edge [Fig. 3(a)]. For Cu, a trough in the interference function occurs at low energies and subtracts from μ_0; this is the cause of a weak feature at the beginning of the edge jump in the Cu-edge calculations, similar to what is seen in the Fe-edge calculations. The low-energy shoulder on the calculated Zn-edge maximum [Fig. 4(a)] is due to similar low-energy features in the MS and SS components that are seen for the Fe- and Cu-edge calculations.

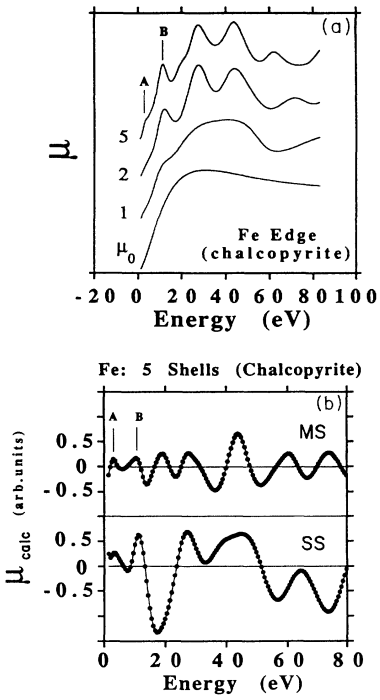

FIG. 3. (a) Fe K-edge calculations from 0 (μ_0) to 5 shells. The pre-edge feature, or feature A, is only present in calculations using four or more shells. (b) Interference contributions to the Fe K-edge calculations. The low-energy features (features A and B) for MS and SS add constructively to produce features on the calculated Fe edge.

Calculation versus data

The E_0's for the experimental data have been shifted to near 0 eV, so that the data best match the calculated spectra (Figs. 4–6). The calculations show that the sharpness of the edge maximum and the energy range of the edge jump are due to the atomic states of the absorber (Fig. 2). The trend of the calculated μ_0 spectra shows that the edge rise takes place over a wider energy range for Cu and Fe (approximately 20 eV), than for Zn (approximately 5 eV). No feature in the calculated μ_0 for the Cu and Fe edges can be attributed to atomic bound-

TABLE II. Contents of the atomic shells around the central absorbing cations used in the ICXANES calculations. Distances from the central absorbing cations (Zn^{2+} in sphalerite, and Cu^{+} and Fe^{3+} in chalcopyrite) are in parentheses measured in Å.

Shell number	Coordinating atom types		
	Zn^{2+}	Cu^{+}	Fe^{3+}
1	4 S (2.34)	4 S (2.30)	4 S (2.25)
2	12 Zn (3.82)	8 Fe (3.73)	4 Fe (3.72)
		4 Cu (3.73)	8 Cu (3.72)
3	12 S (4.48)	8 S (4.33)	8 S (4.35)
		4 S (4.39)	4 S (4.41)
4	6 Zn (5.41)	2 Fe (5.22)	2 Cu (5.22)
		4 Cu (5.29)	4 Fe (5.28)
5	12 S (5.89)	4 S (5.71)	4 S (5.70)
		4 S (5.73)	4 S (5.74)
		4 S (5.75)	4 S (5.78)

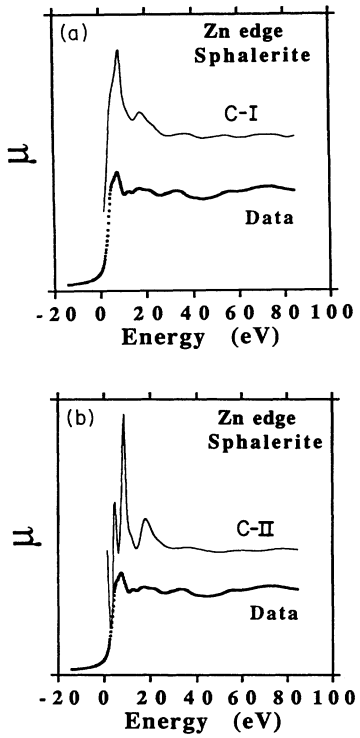

FIG. 4. Calculation (line plot) vs data (points) for the Zn K edge for sphalerite. (a) shows the calculation using Calculational Scheme No. 1, and (b) shows the calculation using Calculational Scheme No. 2. The weighting schemes are given in the text.

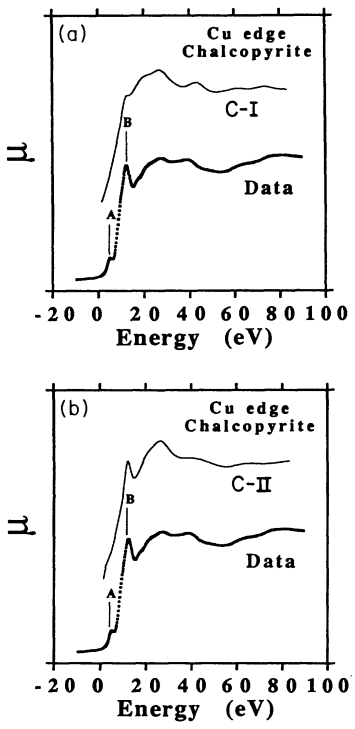

FIG. 5. Calculation (line plot) vs data (points) for the Cu K edge for chalcopyrite. (a) shows the calculation using Calculational Scheme No. 1, and (b) shows the calculation using Calculational Scheme No. 2. Pre-edge and edge features of interest are labeled A and B.

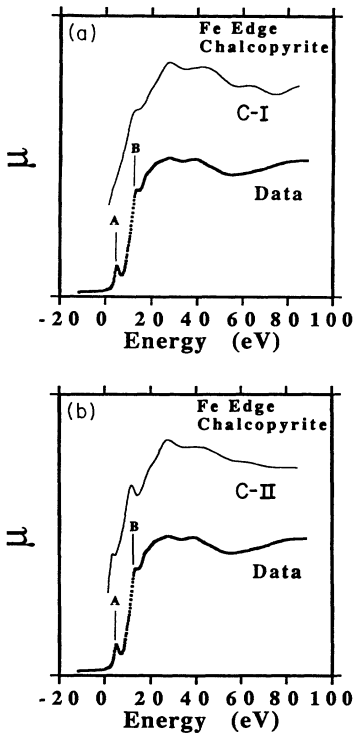

FIG. 6. Calculation (line plot) vs data (points) for the Fe K edge for chalcopyrite. (a) shows the calculation using Calculational Scheme No. 1, and (b) shows the calculation using Calculational Scheme No. 2. Pre-edge and edge features of interest are labeled A and B.

state transitions (Fig. 2) that can lead to pre-edge features in the calculated x-ray-absorption spectrum. The more rapidly varying features on the edges in the calculated x-ray-absorption spectra are due to interference effects from the arrangement of atoms surrounding the absorber.

The calculations generally overestimate the MS and SS amplitudes with respect to the experimental data, especially at energies higher than the edge energy [for Fe, compare Fig. 3(a) top with Fig. 1 bottom]. The interference effects were generally scaled down to have the calculation more closely match the data. Weighting schemes were used to generally damp the amplitude of the interference contributions to the calculated spectra and followed the equation

$$\mu_{\text{calc}} = C_{\text{MS}} f_{\text{MS}}(E) \exp(-\sigma^2_{\text{MS}} k^2) + C_{\text{SS}} f_{\text{SS}}(E) \exp(-\sigma^2_{\text{SS}} k^2) + \mu_0 , \quad (1)$$

where C_{MS} is the multiplicative factor for MS, $f_{\text{MS}}(E)$ is the calculated MS as a function of energy, σ^2_{MS} is the damping factor for MS, k (electron wave vector) is equal to $[4\pi m_e(E-E_0)/h^2]^{1/2}$, C_{SS} is the multiplicative factor for SS, $f_{\text{SS}}(E)$ is the calculated SS as a function of energy, σ^2_{SS} is the damping factor for SS, μ_0 is the atomic contribution from the absorbing cation. In Eq. (1), multiplicative factors C_{MS} and C_{SS} can be considered equivalent to independent s_0^2 values for MS and SS; σ^2_{MS} and σ^2_{SS} can be considered equivalent to independent amplitude-damping

factors that take into account Debye-Waller factor and mean-free-path effects on MS and SS.

No single set of C_{MS}, C_{SS}, σ^2_{MS}, and σ^2_{SS} values could be used to best fit the calculated spectra to the experimental Zn-, Cu-, and Fe-edge data. Two schemes were followed that best matched the calculated spectra to the experimental data. A first set of weighting factors, C_{MS}, C_{SS}, σ^2_{MS}, and σ^2_{SS} were varied so that the weighted calculated Zn-edge spectrum best fit the experimental Zn-edge data; the same weighting factors were then applied to the calculated Cu- and Fe-edge spectra. A second set of weighting factors were varied so that the weighted Fe-edge calculated spectrum best fit the experimental Fe-edge data; these weighting factors were then applied to the calculated Cu- and Zn-edge spectra. The weighting factors that best fit the calculated Zn-edge spectrum to the experimental Zn-edge features did not work as well for the Cu and Fe edges; the weighting factors that best fit the calculated Fe-edge spectrum to the experimental Fe-edge features did work reasonably well for the Cu edge, but did not work well for the Zn edge. Both schemes are about equally successful in reproducing the experimental trends in the interference features, 30 eV and beyond relative to the edge.

The weighted calculated spectrum for the Zn edge that best fit the data [Fig. 4(a), Calculational Scheme No. 1] used the values $C_{MS}=C_{SS}=0.4$, $\sigma^2_{MS}=0.02$ Å^2, and $\sigma^2_{SS}=0.15$ Å^2. Calculational Scheme No. 1 for the Zn-edge calculated spectrum matches reasonably well the features in the experimental Zn-edge data; these results are similar to those in Sainctavit *et al.*[8] The results of Calculational Scheme No. 1 for the calculated Cu and Fe edges do not fit as well the edge features in the experimental data [features *A* and *B* in Figs. 5(a) and 6(a)]. There is virtually no trace of feature *A* for the weighted calculated Cu and Fe edges [Calculational Scheme No. 1 in Figs. 5(a) and 6(a)]. Feature *A* being absent from Calculational Scheme No. 1 weighted Cu- and Fe-edge spectra may mean that the pre-edge feature in the data is due to a bound-state transition which the calculations are not capable of producing.

The weighted calculated spectrum for the Fe edge that best fit the experimental data [Fig. 6(b), Calculational Scheme No. 2] used the values $C_{MS}=4.0$, $C_{SS}=1.0$, $\sigma^2_{MS}=0.38$ Å^2, and $\sigma^2_{SS}=0.15$ Å^2, which enhances MS near the edge, while MS is damped more strongly than SS at energies higher than the edge. Calculational Scheme No. 2 for the calculated Cu and Fe edges better fit the edge features in the experimental data [features *A* and *B* in Figs. 5(b) and 6(b)], than Calculational Scheme No. 1. Features *A* and *B* in Calculational Scheme No. 2 weighted Cu- and Fe-edge spectra are due to interference effects from the crystal structure surrounding Cu and Fe in chalcopyrite. However, this weighting scheme does not work well for the Zn-edge features, since the amplitude of the calculated interference oscillations from 0 to 30 eV are overemphasized compared with the features in the experimental data [Fig. 4(b)]. There is some correspondence though, between the interference features in Calculational Scheme No. 2 weighted Zn-edge spectrum and the experimental Zn-edge data.

CONCLUSIONS

XANES data for Zn, Cu, and Fe in the zinc-blende structure have similar features, except near the edge where the edge maximum decreases in amplitude, while a pre-edge feature appears and increases in amplitude from Zn to Cu to Fe. XANES calculations that incorporate five shells of the crystal structure surrounding the absorbing cations replicate most of the features in the data. Changes in the calculated edge shape for Zn, Cu, and Fe are mostly due to differences in μ_0. The smaller features on and near the calculated edge are due to interference effects from the atomic structure surrounding the absorber. The interference contributions in the calculations were scaled down to specific weighting schemes of MS and SS to best simulate the data. No single weighting scheme could be used to best fit the calculated spectra to the experimental Zn-, Cu-, and Fe-edge data. Two weighting schemes were used to fit the calculated spectra to the experimental data, and two conclusions can be made from the calculations.

The first weighting scheme that does reasonably well fitting the calculated Zn-edge spectrum to features in the experimental Zn-edge data does not do as well for the Fe and Cu edges. The pre-edge feature is not present in the weighted calculated Fe- and Cu-edge spectra. This may indicate that the pre-edge feature in the experimental data is due to bound-state transitions that are not simulated by the calculations. The unexpected presence of the pre-edge feature in the experimental Cu-edge data for chalcopyrite may be due to atomic bound-state transitions that can take place due to hybridization of the filled $Cu^+ 3d$ orbitals with $S^{2-} 3p$ orbitals.

The second weighting scheme that does reasonably well in fitting the calculated Fe-edge spectrum to the experimental Fe-edge data does similarly well for the Cu edge. The low-energy feature, on the weighted calculated Cu- and Fe-edge spectra, is at similar energies relative to the edge and has similar relative intensities compared to the pre-edge feature in the experimental Cu- and Fe-edge data. The low-energy feature on the calculated Cu and Fe edges is due to interference effects from the crystal structure, and is not due to atomic bound-state transitions. These arguments, if applied to the experimental data, are consistent with the electronic configurations for Cu and Fe in chalcopyrite determined by photoemission, Mössbauer, and diffraction studies, where atomic bound-state transitions for Cu^+ are not expected. This weighting scheme overemphasizes the interference effects near the calculated Zn edge compared with the experimental Zn-edge data.

It is interesting to note that one set of the weighted calculated Cu- and Fe-edge spectra have interference features that are at similar energies relative to the edge, and have roughly similar relative intensities compared to the pre-edge features observed in the experimental Cu- and Fe-edge data. These calculations suggest that pre-edge features in the experimental Cu- and Fe-edge data for chalcopyrite, at least, can be due to interference effects from the atomic structure surrounding the absorber, but cannot exclude the possibility that the pre-edge features are due to atomic bound-state transitions

for the absorber.

One way to possibly determine what effect is causing the pre-edge feature in the Cu- and Fe-edge data for chalcopyrite is to gather XANES data for chalcopyrite at various pressures. If the pre-edge features are strictly due to interference effects from the fourth and fifth shells surrounding the absorber, as suggested by the calculations, then small changes in pressure may cause slight shortening of nearest-neighbor distances around the absorber, but should cause larger changes in distance between the absorber and the surrounding fourth and fifth shells. These pressure changes may significantly alter the low-energy MS and SS contributions to the edge, while not significantly altering the local bonding environment of the absorber. If the pre-edge feature changes in position, shape, and intensity at various pressures, then this would indicate that the feature is due to interference effects from the crystal structure; the calculations should be able to follow the trends in the experimental data. If no change is observed in the experimental data, then the pre-edge feature is probably due to atomic bound-state transitions.

ACKNOWLEDGMENTS

I want to thank Dr. J. E. Post and Mr. P. Pohwat of the Mineral Sciences Department of the National Museum of Natural History, Smithsonian Institution for making the mineral samples used in this study available to me.

[1]G. A. Waychunas, M. J. Apted, and G. E. Brown, Phys. Chem. Min. **10**, 1 (1983).

[2]J. L. Shay and J. H. Wernick, *Ternary Chalcopyrite Semiconductors* (Pergamon, New York, 1975), p. 6.

[3]S. R. Hall and J. M. Stewart, Acta Crystallogr. B **29**, 579 (1973).

[4]R. W. G. Wyckoff, *Crystal Structures*, 2nd ed. (Interscience, New York, 1963), Vol. 1, p. 108.

[5]D. A. McKeown, in *X-Ray Absorption Fine Structure*, edited by S. S. Hasnain (Ellis Horwood Publishers, London, 1991), p. 346.

[6]J. Petiau, P. Sainctavit, and G. Calas, Mater. Sci. Engr. B **1**, 237 (1988).

[7]P. Sainctavit, J. Petiau, G. Calas, M. Benfatto, and C. Natoli, J. Phys. C **9**, 1109 (1987).

[8]P. Sainctavit, J. Petiau, M. Benfatto, and C. R. Natoli, Phys. B **158**, 347 (1989).

[9]C. E. Bouldin, R. A. Forman, and M. I. Bell, Rev. Sci. Instrum. **58**, 1891 (1987).

[10]J. A. Tossell, D. S. Urch, D. J. Vaughan, and G. Wiech, J. Chem. Phys. **77**, 77 (1982).

[11]D. J. Vaughan and J. A. Tossell, Phys. Chem. Min. **9**, 253 (1983).

[12]G. Bunker, Ph.D. dissertation, University of Washington, Seattle, 1984.

[13]F. Herman and S. Skillman, *Atomic Structure Calculations* (Prentice-Hall, Englewood Cliffs, NJ, 1963).

[14]K. Schwartz, Phys. Rev. B **5**, 2466 (1972).

[15]L. Mattheiss, Phys. Rev. **134**, A970 (1964).

[16]D. Vvedensky, D. Saldin, and J. Pendry, Comput. Phys. Commun. **40**, 421 (1986).